RESEARCH PAPER

PCCP
www.rsc.org/pccp

Nitrogen dioxide multiphase chemistry: Uptake kinetics on aqueous solutions containing phenolic compounds

Markus Ammann,*[a] Elfriede Rössler,[a] Rafal Strekowski†[b] and Christian George[b]

[a] *Laboratory for Radio and Environmental Chemistry, Paul Scherrer Institute, 5232 Villigen, Switzerland Markus Ammann, OFLA 106, Paul Scherrer Institute, 5232 Villigen, Switzerland. E-mail: markus.ammann@psi.ch; Fax: +41 56 310 4435; Tel: +41 56 310 4049*

[b] *Laboratoire d'Application de la Chimie à l 'Environnement (UCBL-CNRS), 43 boulevard du 11 Novembre 1918, F-69622 Villeurbanne, France. E-mail: christian.george@univ-lyon1.fr; Fax: +33 (0)4 72 44 8114; Tel: +33 (0)4 72 43 1489*

Received 3rd February 2005, Accepted 13th May 2005
First published as an Advance Article on the web 25th May 2005

The uptake coefficients of NO_2 on aqueous solutions containing guaiacol, syringol and catechol were determined over the pH range from 1 to 13 using the wetted wall flowtube technique. The measured uptake coefficients were used to determine the rate coefficients for the reaction of the physically dissolved NO_2 with the neutral and deprotonated forms of phenolic compounds listed above. These organic compounds are ubiquitous not only in biomass burning plumes but also in soils, where they form part of the building blocks of humic acids. The NO_2 uptake kinetics on solutions containing guaiacol, syringol or catechol were observed to be strongly pH dependent with uptake coefficients increasing from below 10^{-7}, under acidic conditions, to more than 10^{-5} at pH values above 10. This behaviour illustrates the difference of reactivity between the neutral phenolic species and the phenoxide ions. The corresponding second order rate coefficients were typically observed to increase from 10^5 M^{-1} s^{-1} for the neutral compounds to a minimum of 10^8 M^{-1} s^{-1} for the phenoxide ions.

Introduction

Lignin is a major structural constituent of vegetation. Microbial degradation or pyrolysis in biomass burning processes, especially in smouldering fires, leads to emissions of a wide range of hydroxy and methoxy substituted aromatic compounds. Catechol, syringol and guaiacol are three major lignin derived metabolites that are representative of this family of compounds and are readily detected in soils (plant litter) and in biomass burning plumes. Their further oxidative degradation leads to radical cations, which in turn undergo polymerization into humic acid type compounds, an important soil forming process[1] and of potential atmospheric importance.[2] Smoke from biomass combustion is one of the largest yet least characterized contributors to atmospheric fine particle levels on local, regional and global scales.[3,4] Catechol (*o*-dihydroxybenzene), guaiacol (*o*-methoxyphenol), syringol (2,6-dimethoxyphenol) and similar compounds have been detected in biomass burning plumes[5] or ambient air influenced by corresponding anthropogenic activities, *e.g.*, residential fires.[6] Individual ratios of these species to CO have been estimated about 10^{-4} in wild fire emissions.[7] In soils, capillary water within the top organic soil layer contains typically between 0.1 and 1 mg l^{-1} of phenolic monomers and about 10 mg l^{-1} of phenols in total (including polyphenols).[8]

In aqueous solution, nitrogen dioxide (NO_2) may undergo electron transfer reactions with phenoxide anions, which have been previously investigated for methylphenols and hydroxybenzenes,[9] catechins[10] and hydroxycinnamic acid derivatives.[11] The primary reactant is the deprotonated species, the phenoxide ion, leading to strongly pH dependent overall kinetics.

The primary reaction products of gaseous NO_2 with these organic compounds are the corresponding phenoxy type radical (or the corresponding radical cations) or nitrite anions. In an acidic aqueous environment, the nitrite ion may be subsequently protonated and released to the gas phase as HONO, or undergo secondary chemistry, eventually leading to NO and/or N_2O[12,13] or nitrated organics. In atmospheric chemistry, HONO plays an important role as an OH radical source due to its photolysis.[14] Field studies indicate that HONO is mainly formed heterogeneously from NO_2 on ground or airborne surfaces such as aerosol particles and cloud droplets. Previous modelling studies have mostly considered the self-reaction of NO_2 in an aqueous solution as a source of HONO on humid surfaces, the kinetics of which, however, is relatively slow. Recent field measurements also indicate substantial day-time HONO concentrations possibly due to hitherto unknown photochemistry on the ground, rendering HONO an even more significant day-time OH source.[15–17]

In a recent study, we have reported measurements of NO_2 uptake into solutions of *m*-dihydroxybenzene (resorcinol) and 2,7-dihydroxynaphthalene, both occurring as photo-oxidation products of aromatic compounds in the atmosphere, in the pH range from 3 to 11 using the wetted wall flowtube technique.[18] In a multiphase modelling study, we have addressed the atmospheric impact of these reactions, as far as their kinetics was known at that time, on the levels of HONO in the gas phase and nitrite in the aerosol phase under typical urban conditions.[19] That study indicated that the significance of these reactions depends heavily on the total amount of aromatics appearing in the aqueous phase and on aerosol pH. Therefore, in environments with a high content of these compounds combined with the presence of neutralizing minerals, such as in an aerosol from burning of biomass or above soils, a much higher impact of these species on HONO or nitrite may be expected. In the present study, we have expanded our kinetic

† Present address: Université de Provence, TRACES, Centre de Saint Jérôme, Case 512, 13397 Marseille Cedex 20, France. E-mail: Rafal.Strekowski@up.univ-mrs.fr; Tel: (+33) (0)4 91 28 89 00.

DOI: 10.1039/b501808k

experiments to three major lignin derived metabolites *i.e.*, guaiacol, syringol and catechol.

Experimental

Wetted-wall flowtube technique

The uptake of gaseous NO_2 into aqueous solutions containing guaiacol, syringol or catechol was studied using the wetted wall flowtube (WWFT) technique.[20–24] Experiments reported here were conducted in both involved laboratories using two very similar set-ups. Where necessary, the setups operated in Lyon, France, and Villigen, Switzerland, will be referred to as LACE and PSI, respectively. The WWFT is a well established experimental approach that has been used to study the transport of gases into liquids for many years [for further examples see ref. 25 and references therein]. The WWFT method takes advantage of the fact that the well described mass transport equation in cylindrical co-ordinates can be applied. The uptake kinetics were determined from the measured loss rate of gas-phase NO_2 flowing along a vertically aligned flowtube, the wall of which was covered by a film of an aqueous solution allowed to flow slowly under the effect of gravity. Thereby, the observed loss of NO_2 from the gas phase is used to obtain the reactive uptake coefficient, defined as the probability that a gas kinetic collision of a gaseous NO_2 molecule with the liquid surface leads to reactive loss within the liquid. At the bottom of the tube, the reagent solution is pumped out to waste or to a sample vial for further analysis.

The instruments operated in our laboratories have been described in detail in our previous studies for PSI[18,26] and LACE[18,26] and are designed for the measurement of uptake coefficients in the range of 10^{-5} to 10^{-8} at ambient pressure.

The NO_2 reactant gas concentration was measured at the exit of the flowtube as a function of the distance (time) that the NO_2 gas was in contact with the aqueous film. The NO_2 reactant gas was monitored using a quadrupole mass analyser (at LACE) or a chemiluminescence detector (Monitorlabs, ML9841) (at PSI). The use of different detectors is accompanied with different NO_2 working concentrations. The latter were in the range 10–100 ppm for the MS experiments (LACE) and 10–100 ppb for the chemiluminescence experiments (PSI). In both cases, the NO_2 concentrations were obtained by diluting a certified NO_2 gas mix with the appropriate carrier gas.

Under the typical experimental conditions used for the concentration of the NO_2 gas, the NO_2 dimer (*i.e.*, N_2O_4) is not expected to play a major role in the uptake kinetics. This was confirmed by varying the NO_2 gas phase concentrations. No difference in the uptake was observed.

The solutions used to produce the aqueous film were prepared by allowing a known quantity (weight or volume) of the organic compound to be dissolved in a known volume of water. Under the typical experimental conditions employed the organic solution concentrations used were in the range 10^{-5} to 10^{-1} mol L^{-1}. The freshly prepared standard organic solutions were used without further analysis.

At PSI, the reagent solutions were prepared with degassed Millipore water located in a glovebag continuously flushed with nitrogen (99.999%) to avoid any contact of the solution with oxygen, prior to the reaction. The solutions were pumped to the WWFT directly from within the glovebag. At PSI, the pH values between 6 and 11 were set using phosphate buffers, values below pH 6 were prepared using sulfuric acid, values of 13 were adjusted using potassium hydroxide. The pH of the effluent solutions was routinely checked directly at the exit of the flowtube. The buffers had no effect on the NO_2 uptake (see results).

At LACE, the pH of the solutions were adjusted by adding either sulfuric acid or sodium hydroxide but were not buffered, nor degassed, in order to address the uptake kinetics under different conditions than those used at PSI.

In this study, only the gas phase was analysed *i.e.*, the appearance of nitrite ions could not be monitored.

As the selected approach is based on flow experiments, the aqueous film was constantly and rapidly (within seconds) renewed preventing accumulation of reaction products. It is therefore assumed that the latter are not affecting our kinetic experiments. Again the absence of effect due to changes in the gas phase concentration of NO_2 is supporting this assumption.

The schematic of the experimental approach is shown in Fig. 1. Some experimental details that are relevant to this work are given below. An upright Pyrex tube with an internal volume of approximately 314 cm^3 was used in all experiments. The Pyrex reactor was about 100 cm (LACE) and 60 cm (PSI) long, and the inner diameter was 1.0 cm (LACE) and 1.2 cm (PSI). It was maintained at a constant temperature (298.0 ± 0.5 K) by circulating a 1 : 1 ethanol + methanol mixture from a thermostatically controlled bath through the outer jacket. The reactant NO_2 gas and the carrier gas (nitrogen for PSI and helium for LACE) were introduced into the reactor *via* a static 9.5 mm od Teflon insert that has been mechanically fitted to leave a space of less than 0.5 mm between its outer diameter and the inner wall of the reactor. This allowed for a little reservoir of the aqueous solution to be formed just above the inner reactor tube. A peristaltic pump was used to pump the aqueous solution into the reservoir. Once enough liquid accumulated in the reservoir, gravity allowed for the aqueous solution to fall and coat the inner wall of the reactor. This point is discussed in detail in the section below. The gases were extracted from the flowtube by a moveable outlet (6 mm od).

Water vapour was added to the total flow by allowing the carrier gas to pass through a flask containing deionized H_2O. Controlling humidity in the wetted wall reactor was necessary to avoid any potential evaporation of water from the falling liquid film that could in turn result in cooling.

Uptake coefficients

The flow dynamics of a liquid film allowed to fall under the effect of gravity in a cylindrical tube has already been discussed

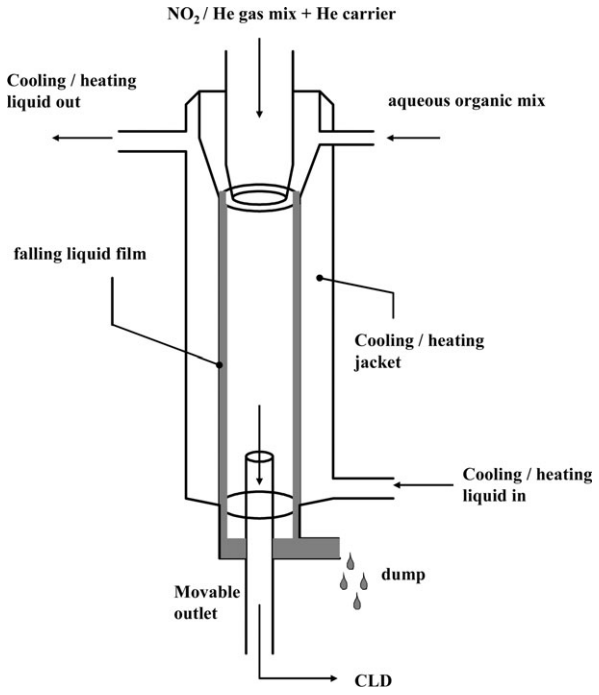

Fig. 1 Schematic representation of the vertically mounted wetted-wall reactor used to measure the uptake of NO_2 on aqueous films.

in detail by Danckwerts.[20] The thickness of the film f was calculated using the following eqn. (1).

$$f = \left(\frac{3\eta F_l}{\pi g d_{tube}\rho}\right)^{1/3} \quad (1)$$

In eqn. (1) above, η, ρ and F_l are the viscosity, density and liquid flow rate of the falling liquid film, respectively. Under typical experimental conditions employed in this work the liquid flow rate was in the range 2–6 ml min^{-1} and the resulting film thickness was in the range from 6.1×10^{-3} to 1.2×10^{-2} cm.

In order to ensure that the mass transport in the gas phase is described by molecular diffusion processes alone, *i.e.*, without the effects of turbulence possibly produced by the film's surface ripples, the falling liquid flow has to be laminar. This was ensured by keeping the liquid flow rates as low as possible. Under the experimental conditions employed in this work the presence of ripples on film surfaces was never observed. Another indicator for the presence of turbulence in the liquid film is described by the Reynolds' number, N_{Re} [eqn. (2)].

$$N_{Re} = \frac{F_l \rho}{\pi d_{tube}\eta} \quad (2)$$

In this work, the calculated Reynolds' number was smaller than 3, a value far below the limit of 250–400 where turbulent transport is favoured. Therefore, it was assumed that gas phase transport can be described by diffusion alone.

The trace gas loss rate in the flowtube can be measured as a function of the position (distance) of the movable outlet *i.e.*, as a function of the gas/liquid exposure time t. The length l of the interaction zone can be varied up to $l = 80$ cm at LACE and $l =$ 40 cm at PSI. The entrance section (10 cm) of the flowtube, where the laminar flow profile and gas-liquid equilibration occurs, was never used for analysis.

$$\frac{n - \Delta n}{n} = \exp[-k_w t] \quad (3)$$

As shown in eqn. (3) above, the loss rate can be described with a first order rate law with respect to the gas phase concentration of the reactant. In eqn. (3) t is the average gas residence time and k_w is the first order rate coefficient for the reaction at the liquid film surface. We assume in eqn. (3) that the loss rate can be described with a first order rate law. To a first approximation the rate coefficient k_w can be calculated by integrating both sides of eqn. (3) above.

$$k_w = \frac{\gamma\langle c\rangle}{2r_{tube}} \quad (4)$$

In eqn. (4), r_{tube}, γ, and $\langle c\rangle$ are the flowtube radius, uptake coefficient and average molecular velocity, respectively. However, eqn. (4) does not hold if gas phase diffusion limitations are present, *i.e.*, when radial gas concentration profiles build up. To take into account gas phase diffusion, the Cooney–Kim–Davis (CKD) eqn. (5)[27] was used as described in detail by Behnke and co-workers:[28,29]

In eqn. (5) above, B_i and Λ_i are functions of the Sherwood number N_{shw} [see eqn. (6) below] and z^* is a dimensionless reaction length.

$$N_{shw} = \frac{r_{tube}\langle c\rangle}{4D_g}\left(\frac{\gamma}{1 - \gamma/2}\right) \quad (6)$$

In eqn. (6), γ is the corrected uptake coefficient. The dimensionless reaction length z^* can be calculated using eqn. (7) listed below, where l is the reaction length, D_g is the binary gas diffusion coefficient, T is the temperature and F_g is the gas flow rate (cm^3 s^{-1}), which was in the range from 3–8 cm^3 s^{-1} and 5.8 cm^3 s^{-1} for LACE and PSI, respectively.

$$z^* = l\frac{D_{g,0}}{2F_g^0}\frac{T}{T_0} \quad (7)$$

The subscript '0' refers to standard conditions. Values of B_i and Λ_i were taken from the table reported by Murphy and Fahey[21] and interpolated from the four nearest values of N_{shw} using a cubic polynomial.

Applying eqn. (5) to the results obtained in this work was shown to give results in excellent agreement with the mathematical approach developed by Brown *et al.*[30] Comparison of the method given by eqn. (5) with the simple exponential approach given by eqn. (3) was used to check to what degree uptake coefficients obtained in this work were affected by gas phase diffusion limitations. For the PSI experiments, where the highest measured values for the uptake coefficients were around 10^{-5}, the deviation from the simple exponential behaviour induced by diffusion in the gas phase was observed to be about 20% (*i.e.*, once corrected, the uptake coefficient increased by 20%). For the LACE experiments, the observed deviation was observed to be mostly below 5%. This difference is believed to be mainly due to different carrier gases used, *i.e.*, helium and nitrogen, for the LACE end PSI experiments, respectively. Gas phase diffusion proceeds at higher rates in helium than in nitrogen. Nevertheless, all experimental results presented below have either not been affected by gas phase limitations or have been corrected for the effect of slow gas phase diffusion. Note that we have cross-checked the overall procedure by performing the experiments with ABTS (2,2′-azino-bis(3-ethylbenzthiazoline-6-sulfonic acid) for reference using the PSI setup.

Results

All results listed in this section were obtained at 298 K.

The flowtube technique used in this work in principle allows for sensitive measurements of very small uptake coefficients (as low as a few times 10^{-8}). Accordingly, uptake of the poorly water soluble NO_2 into pure water was detectable, always with uptake coefficients on the order of 10^{-7} or below. This is due to the slow hydrolysis reaction of NO_2, which proceeds through a complex reaction mechanism. Also, due to its second-order character, the uptake coefficient of NO_2 is depending on its gas phase concentration, increasing the complexity of this system. As these experiments were performed with the MS experiments (*i.e.*, with high NO_2 concentrations of about 50 ppm), they were certainly much influenced by this second order chemistry. Uptake of NO_2 by water has been previously studied in more detail,[31] and it is not our aim to provide here more insights into this complex chemistry. We underline that the uptake coefficients of NO_2 on water, as observed in the course of these experiments, were always smaller (by at least a factor 5) than those measured on aqueous solutions containing organic compounds described below, at all pH. Note also that for the experiments at PSI, which were performed at much lower NO_2 concentration, the low uptake coefficient of 10^{-7} and below on the aqueous solutions without organics was confirmed at each pH. Each series of measurements at different concentrations of the organic compound was followed by one with the pure buffer solution (after thoroughly cleaning the flowtube).

Uptake on solutions containing aromatics

The chemical system becomes (apparently) simpler when adding increasing concentrations of phenolic compounds to the aqueous solution. Fig. 2 shows the uptake coefficients of NO_2 on catechol containing solutions at different pH. It is obvious that the uptake rate is drastically increased compared to water, which means that this compound introduces a new reactive pathway (in the solution) that enhances the uptake of NO_2.

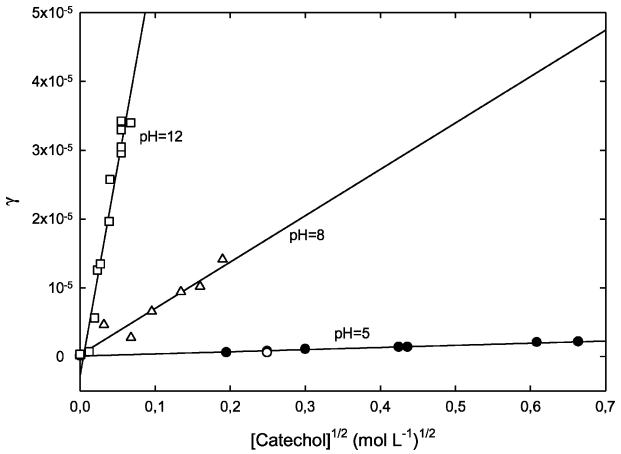

Fig. 2 Uptake coefficients measured on catechol solutions as a function of its concentration and pH. These data were obtained at LACE at 298 K with a NO_2 concentration of 90 ppm (open symbols) or 30 ppm (closed circles).

Apart from the disproportionation reaction mentioned, the following three reactions of the phenolic compounds (named generically as ArOH) have to be considered for the present system:

$$NO_2 + ArOH \rightarrow HONO + ArO^{\bullet} \qquad (R1)$$

$$NO_2 + ArO^- \rightarrow NO_2^- + ArO^{\bullet} \qquad (R2)$$

where ArOH is the undissociated form of the phenolic compounds, ArO^- is the deprotonated form.

The following simplified equation can be applied to our data, if the uptake without added ArOH is negligible, in order to extract $Hk^{1/2}$ values:[32]

$$\gamma = \frac{4HRT\sqrt{kD}}{\langle c \rangle} \qquad (8)$$

where H is the NO_2 Henry's law constant, R the gas constant, D the NO_2 aqueous phase diffusion coefficient, T the temperature and k is the pseudo-first order rate constant. Equation (8) is also based on the assumption of an uptake proceeding at steady-state but does not require attainment of the Henry's law equilibrium over the entire depth of the film. It assumes however an equilibrated surface concentration, which is rapidly attained.

Fig. 2 shows a plot of the uptake coefficient *versus* the square root of the concentration of the NO_2 scavenger (*i.e.*, catechol in this particular case) according to eqn. (8). It can be seen that the uptake coefficients exhibit indeed a linear dependence that almost goes through the origin of such a plot. This shows that the uptake is effectively and exclusively driven by the reaction of NO_2 with the aromatics *i.e.*, there is no competition with the hydrolysis described shortly above. Indeed, all uptake coefficients on aromatic containing solutions were at least a factor of 5 higher than on water (under the same experimental conditions employed). Based on the second order rate coefficient reported by Cheung *et al.*,[31] the first order loss rate constant of NO_2 due to the hydrolysis reaction is at least a factor of 10 less than the loss rate constant derived from the observed uptake coefficient, which was due to reactions (R1) and (R2).

Under the conditions chosen in this study, uptake into the liquid was limited by the combined effects of reaction and diffusion in the liquid phase. It was assumed that the mass accommodation coefficient, α is much larger than the uptake coefficient, γ. Then, the overall second order rate constant k_X^{II} for reactions (R1) and (R2) in the aqueous phase was calculated from the measured γ values using eqn. (9):

$$k_X^{II} = \left[\frac{\gamma \frac{\langle c \rangle}{4}}{H_{NO_2} RT}\right]^2 \frac{1}{[X] D_{NO_2}} \qquad (9)$$

where k_X^{II} denotes the overall second order rate constant in the liquid phase, [X] the concentration of the liquid phase reactant, H_{NO_2} the Henry's law constant for NO_2 (0.014 M atm^{-1},[33] $\langle c \rangle$ its mean thermal molecular velocity (37 000 cm s^{-1} at 298 K). D_{NO_2} is the diffusion coefficient in the liquid phase (1.23×10^{-5} cm^2 s^{-1}.[33] We used ABTS (2,2′-azino-bis(3-ethylbenziazoline-6-sulfonic acid) (as reference to check the overall procedure and) obtained a value of k_{II} of 2.48×10^7 (9.4×10^6) M^{-1} s^{-1} in the pH range of 1 to 9, which is in good agreement with the often used literature value of 2.2×10^7 M^{-1} s^{-1} in the pH range of 6.5 to 9.[34]

Fig. 3 shows a compilation of the uptake coefficients γ of NO_2 into ArOH containing solutions as a function of ArOH concentration and pH for all compounds measured at PSI. No dependence of γ of the NO_2 concentration was observed in the range of 20 to 2000 ppbv of NO_2. The values of the uptake coefficients are contained in the range from 2×10^{-7} to 6×10^{-5} for the whole set of experiments. Fig. 3 also contains the data obtained at LACE for catechol at pH = 12 (open stars at concentrations larger than 10^{-4} mol L^{-1}). It can be seen that they fit reasonably well to the PSI data at the same pH. As the experiments made at LACE were done at higher NO_2 concentration with unbuffered solutions they potentially carry a large uncertainty in the solution pH. Therefore, these data were not considered for the calculation of the aqueous phase second order rate constants performed below.

As given in eqn. (9), under the assumption of uptake limited by diffusion in the liquid phase, γ is proportional to the square root of the ArOH concentration, resulting in a slope of 1/2 on the double logarithmic plot of Fig. 3, indicated by the parallel solid lines. The fact that in most cases the same symbols plot parallel to these lines indicates that the data are in agreement with this assumption. An exception seem to be the data points obtained at pH 1, where secondary reactions of HONO (decomposition into NO and NO_2) might have led to an underestimation of γ. For syringol, at pH 1, the fits of eqn. (5) to the observed loss curves showed some deviation from the

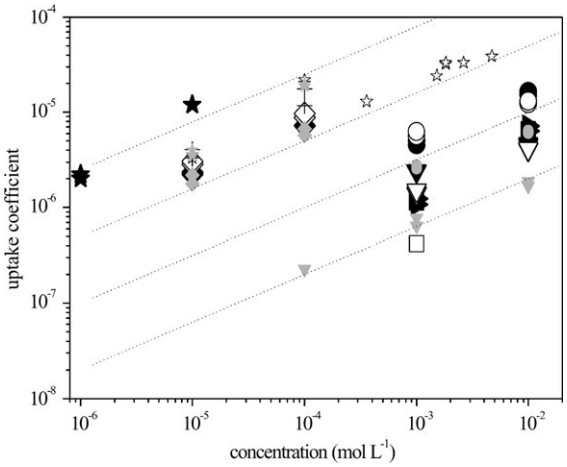

Fig. 3 Uptake coefficient γ at the aqueous surface (after correction for diffusion in the gas phase), measured at 298 K, plotted as a function of aqueous phase concentration of ArOH. The black solid, black open and grey solid symbols refer to syringol, catechol and guaiacol, respectively. The symbol types refer to the pH of the aqueous solution: (△) pH = 1, (□) pH = 3, (▽) pH = 6, (○) pH = 7, (◇) pH = 9, (★) pH = 12, (☆) pH = 13. The dotted lines indicate the slope of the square root dependency expected for uptake limited by diffusion in the liquid phase.

Table 1 Overview of reactions and measured rate constants

	Species		CAS no.	Reaction	$k^{II}/M^{-1}\ s^{-1}$ or pK published values	This work
	Catechol	1,2-Dihydroxy benzene	120-80-9	$C_6H_4(OH)_2 + H_2O = C_6H_4(OH)O^- + H_3O^+$	p$K_1 = 9.3^a$	9.1
1a				$C_6H_4(OH)_2 + NO_2 = C_6H_4(OH)O + HONO$	$k_{1,1}$	1×10^4
1b				$C_6H_4(OH)O^- + NO_2 = C_6H_4(OH)O + NO_2^-$	$k_{1,2}$	1.3×10^8
	Guaiacol	2-Methoxyphenol	90-05-1	$C_6H_4(OCH_3)OH + H_2O = C_6H_4(OCH_3)O^- + H_3O^+$	p$K_2 = 9.9^b$	9.8
2°				$C_6H_4(OCH_3)OH + NO_2 = C_6H_4(OCH_3)O + HONO$	$k_{2,1}$	$<10^4$
2b				$C_6H_4(OCH_3)O^- + NO_2 = C_6H_4(OCH_3)O + NO_2^-$	$k_{2,2}$	1.5×10^8
	Syringol	2,6-Dimethoxyphenol	91-10-1	$C_6H_3(OCH_3)_2OH + H_2O = C_6H_3(OCH_3)_2O^- + H_3O^+$	p$K_3 = 10.2^c$	9.8
3°				$C_6H_3(OCH_3)_2OH + NO_2 = C_6H_3(OCH_3)O + HONO$	$k_{3,1}$	1.5×10^5
3b				$C_6H_3(OCH_3)_2O^- + NO_2 = C_6H_3(OCH_3)O + NO_2^-$	$k_{3,2}$	4.5×10^8
4b	Quinol	1,4-Benzenediol	123-31-9	$C_6H_4(OH)O^- + NO_2 = C_6H_4(OH)O + NO_2^-$	$k_{4,2} = 1.1 \times 10^9$ [d]	
5b	*m*-Guaiacol	3-Methoxyphenol	150-19-6	$C_6H_4(OCH_3)O^- + NO_2 = C_6H_4(OCH_3)O + NO_2^-$	$k_{5,2} = 1.8 \times 10^7$ [e]	
6b	Mequinol	4-Methoxyphenol	150-76-5	$C_6H_4(OCH_3)O^- + NO_2 = C_6H_4(OCH_3)O + NO_2^-$	$k_{6,2} = 2.1 \times 10^8$ [f]	
7b	Resorcinol	1,3-Benzenediol	108-46-3	$C_6H_4(OH)O^- + NO_2 = C_6H_4(OH)O + NO_2^-$	$k_{7,2} = 1.3 \times 10^7$ [g]	

[a] Ref. 36; other literature range 9.0–9.5. [b] Ref. 37; other literature range 9.2–10.0. [c] Ref. 38. [d] Ref. 9. [e] Ref. 9. [f] Ref. 39. [g] Ref. 40.

behaviour expected for a simple first order loss process at the surface.

An obvious factor strongly affecting the uptake coefficient is the pH of the solutions. Increasing the pH led to higher uptake coefficients, as this was previously reported for other compounds. This is due to the increasing fraction of the more reactive deprotonated species at higher pH. To include the acid–base equilibria in the second order rate constant, k_X^{II} can also be expressed as a superposition of the rate constants of the neutral and deprotonated species, respectively:

$$k_X^{II} = (1 - \theta_{X_1})k_{X_1} + \theta_{X_1}k_{X_2} \qquad (10)$$

θ_X denotes the fraction of X, which is deprotonated at a given pH (see Table 1 for published pK values). Knowing the values of pK_a for the acids, the relative amount θ_Ξ of the singly dissociated species at a certain pH can be calculated using the Henderson–Haselbalch formula:[35]

$$\theta_1 = \frac{1}{1 + 10^{(pK_{a1} - pH)}} \qquad (11)$$

Eqn. (10) was used to fit the k_{II}^X values as a function of pH with k_X^1, k_X^2 and pK_X as adjustable parameters.

k_X^{II} values obtained from the measured uptake coefficients are plotted in Fig. 4. The reactivity obviously follows deprotonation as a function of pH due to the orders of magnitude higher reactivity of the deprotonated species than the neutral species. The solid lines in Fig. 4 are a fit of eqn. (10) to the measured data. The data at lowest and highest pH allowed to constrain mostly k_{X_1} and k_{X_2}, respectively, whereas the data at intermediate pH are most sensitive to the pK_X value. The results are given in Table 1. The pK values are clearly in agreement with previously reported values. The rate constants for the monoanions are also in the range of those few structurally similar species already reported in the literature, which are summarized in Table 1 for comparison.

Conclusions and atmospheric implications

Using the wetted wall flowtube technique, the uptake rates and liquid phase kinetics of catechol, syringol and guiacol with NO_2 were investigated over the pH range 1 to 13 and for different initial reactant concentrations. These substances serve as reactants in the reduction of NO_2 to nitrite, which is the liquid phase base associated to atmospheric nitrous acid. The results were interpreted using a simple model taking into account the deprotonation of these three weak organic acids. The present results might serve as input into atmospheric box model aiming at assessing the importance of heterogeneous HONO formation due to semi-volatile organic compounds as postulated in one of our recent studies.[41] Also these kinetics support the outcomes of an exploratory study by Lahoutifard *et al.*,[19] where a multiphase model was applied to simulate the chemistry of dissociated hydroxyl-substituted aromatics occurring in liquid aerosol particles, in the early morning, under polluted conditions. That chemistry produces nitrite ions in the liquid phase with kinetics (that were almost missing at the time of their study), which, depending on the pH, may lead to HONO out-gassing. The strength of this source was explored, and it was shown that it leads to HONO even for very dilute liquid droplets under moderate acidic conditions, and increases in importance when the aromatic content of the droplets is increased. The influence of these reactions on daytime photo-

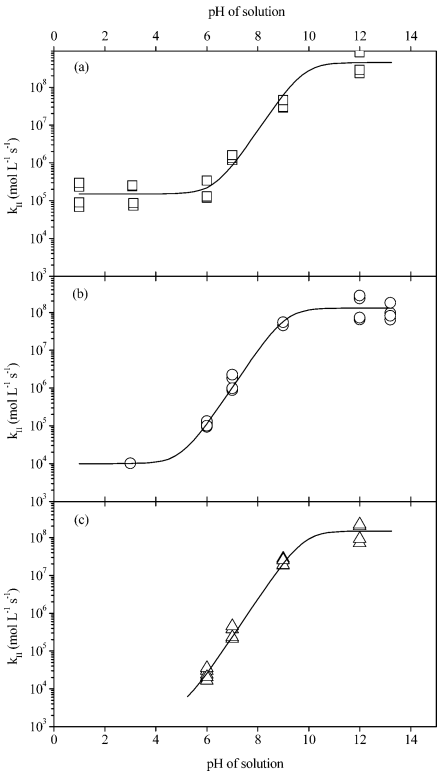

Fig. 4 Overall aqueous phase second order rate constant of NO_2 with ArOH solution plotted as a function of pH. Squares, circles, triangles refer to syringol, catechol, guaiacol, respectively. The solid lines were obtained by fitting eqn. (14) to the measured data.

chemistry is still minor with a notable impact only at heavily polluted locations or in biomass burning plumes, in which the title compounds may represent about 1% of water soluble organic aerosol mass [5]. On the other hand, structurally similar compounds are also present in the soil water with concentrations in the 10 mg l^{-1} (10^{-4} M) range at typical soil water pH of 4 to 5.[8] Uptake coefficients of NO_2 into such an aqueous phase of 10^{-6} seem reasonable (see Fig. 3) and by far exceed that for the heterogeneous hydrolysis of NO_2. It remains to be investigated to what degree the non-aqueous soil fraction contributes to this chemistry as these phenolic species may also occur in adsorbed form on minerals and humic acids, or form even part of the latter.[1] Some insight into this may be derived from the study by Arens *et al.*[41] on solid 1,2,10-trihydroxyanthracene, on which HONO formation scaled with the relative humidity with uptake coefficients also in the 10^{-6} range.

Acknowledgements

The support by the French program PRIMEQUAL2 for the project SHONO and by the Swiss National Science Foundation are gratefully acknowledged.

References

1 K. H. Tan, *Humic matter in soil and the environment: principles and controversies*, Marcel Dekker, Inc, New York, Basel, 2003.
2 A. Hoffer, G. Kiss, M. Blazso and A. Gelencser, *Geophys. Res. Lett.*, 2004, **31**, L06115, DOI: 10.1029/2003GL018962.
3 W. F. Rogge, L. M. Hildemann, M. A. Mazurek, G. R. Cass and B. R. T. Simoneit, *Environ. Sci. Technol.*, 1998, **32**, 13.
4 O. L. Mayol-Bracero, P. Guyon, B. Graham, G. Roberts, M. O. Andreae, S. Decesari, M. C. Facchini, S. Fuzzi and P. Artaxo, *J. Geophys. Res., [Atmos.]*, 2002, **107**, 8091, DOI: 10.1029/2001JD000522.
5 B. Graham, O. L. Mayol-Bracero, P. Guyon, G. C. Roberts, S. Decesari, M. C. Facchini, P. Artaxo, W. Maenhaut, P. Koll and M. O. Andreae, *J. Geophys. Res., [Atmos.]*, 2002, **107**, art. no.
6 B. R. T. Simoneit, J. J. Schauer, C. G. Nolte, D. R. Oros, V. O. Elias, M. P. Fraser, W. F. Rogge and G. R. Cass, *Atmos. Environ.*, 1999, **33**, 173.
7 L. M. McKenzie, W. M. Hao, G. N. Richards and D. E. Ward, *Environ. Sci. Technol.*, 1995, **29**, 2047.
8 C. Gallet and C. Keller, *Soil Biol. Biochem.*, 1999, **31**, 1151.
9 Z. B. Alfassi, R. E. Huie and P. Neta, *J. Phys. Chem.*, 1986, **90**, 4156–4158.
10 J. L. Miao, W. F. Wang, J. X. Pan, C. Y. Lu, R. Q. Li and S. D. Yao, *Radiat. Phys. Chem.*, 2001, **60**, 163.
11 Z. Zhan, S. Yao, W. Lin, W. F. Wang, Y. Jin and N. Lin, *Free Radical Res.*, 1998, **29**, 13.
12 J. Kleffmann, K. H. Becker and P. Wiesen, *J. Chem. Soc., Faraday Trans.*, 1998, **94**, 3289.
13 J. Baker, S. F. M. Ashbourn and R. A. Cox, *Phys. Chem. Chem. Phys.*, 1999, **1**, 683.
14 R. M. Harrison, J. D. Peak and G. M. Collins, *J. Geophys. Res.*, 1996, **101**, 14429.
15 B. Aumont, F. Chervier and S. Laval, *Atmos. Environ.*, 2003, **37**, 487.
16 J. Kleffmann, R. Kurtenbach, J. Lörzer, P. Wiesen, N. Kalthodd, B. Vogel and H. Vogel, *Atmos. Environ.*, 2003, **37**, 2949.
17 B. Vogel, H. Vogel, J. Kleffmann and R. Kurtenbach, *Atmos. Environ.*, 2003, **37**, 2957.
18 L. Gutzwiller, C. George, E. Rössler and M. Ammann, *J. Phys. Chem. A*, 2002, **106**, 12045.
19 N. Lahoutifard, M. Ammann, L. Gutzwiller, B. Ervens and C. George, *Atmos. Chem. Phys.*, 2002, **2**, 215.
20 P. V. Danckwerts, *Gas-Liquid Reactions*, McGraw-Hill, New York, 1970.
21 D. M. Murphy and D. W. Fahey, *Anal. Chem.*, 1987, **59**, 2753.
22 D. R. Hanson and A. R. Ravishankara, *Geophys. Res. Lett.*, 1995, **22**, 385.
23 V. Scheer, A. Frenzel, W. Behnke, C. Zetzsch, L. Magi, C. George and P. Mirabel, *J. Phys. Chem. A*, 1997, **101**, 9359.
24 S. Fickert, F. Helleis, J. W. Adams, G. K. Moortgat and J. N. Crowley, *J. Phys. Chem. A*, 1998, **102**, 10689.
25 B. J. Finlayson-Pitts and J. N. Pitts, *Chemistry of the Upper and Lower Atmosphere: Theory, Experiments and Applications*, Academic Press, San Diego, FL, 2000.
26 R. S. Strekowski and C. George, *J. Chem. Eng. Data*, 2005, **50**, 804.
27 D. O. Cooney, S. Kim and E. J. Davis, *J. Chem. Eng. Sci.*, 1974, **29**, 1731.
28 W. Behnke, H. U. Krüger, V. Scheer and C. Zetzsch, *J. Aerosol Sci.*, 1992, **S23**, 933.
29 W. Behnke, C. George, V. Scheer and C. Zetzsch, *J. Geophys. Res.*, 1997, **102**, 3795.
30 S. S. Brown, R. W. Wilson and A. R. Ravishankara, *J. Phys. Chem. A*, 2000, **104**, 4976.
31 J. L. Cheung, Y. Q. Li, J. Boniface, Q. Shi, P. Davidovits, D. R. Worsnop, J. T. Jayne and C. E. Kolb, *J. Phys. Chem. A*, 2000, **104**, 2655.
32 C. E. Kolb, D. R. Worsnop, M. S. Zahniser, P. Davidovits, D. R. Hanson, A. R. Ravishankara, L. F. Keyser, M. T. Leu, L. R. Williams, M. J. Molina and M. A. Tolbert, in *Advances in Physical Chemistry Series*, ed. J. R. Barker, World scientific, Singapore, 1994, Vol. 3.
33 J. L. Cheung, Y. Q. Li, J. Boniface, Q. Shi, P. Davidovits, D. R. Worsnop, J. T. Jayne and C. E. Kolb, *J. Phys. Chem. A*, 2000, **104**, 2655.
34 L. G. Forni, V. O. Mora-Arellano, J. E. Packer and R. L. Willson, *J. Chem. Soc., Perkin Trans.*, 1986, **II**, 1.
35 A. Albert and E. P. Serjeant, *The Determination of Ionization Constants*, Chapman and Hall, London and New York, 1984.
36 A. Kimura *et al.*, *J. Am. Chem. Soc.*, 1983, **105**, 2063–2066.
37 Z. B. Alfassi and R. H. Schuler, *J. Phys. Chem.*, 1985, **89**, 3359–3363.
38 E. Chapoteau, B. P. Czech, A. Kumar, A. Pose, R. A. Bartsch, R. A. Holwerda, N. K. Dalley, B. E. Wilson and W. Jiang, *J. Org. Chem.*, 1989, **54**, 861–867.
39 Z. B. Alfassi, R. E. Huie, P. Neta and L. C. T. Shoute, *J. Phys. Chem.*, 1990, **94**, 8800–8805.
40 L. Gutzwiller, C. George, E. Rössler and M. Ammann, *J. Phys. Chem.*, 2002, **106**, 12045.
41 F. Arens, L. Gutzwiller, H. W. Gaggeler and M. Ammann, *Phys. Chem. Chem. Phys.*, 2002, **4**, 3684.

